nature genetics

Root tip contact with low-phosphate media reprograms plant root architecture

Sergio Svistoonoff[1,2], Audrey Creff[1], Matthieu Reymond[1,3], Cécile Sigoillot-Claude[1], Lilian Ricaud[1], Aline Blanchet[1,4], Laurent Nussaume[1] & Thierry Desnos[1]

Plant roots are able to sense soil nutrient availability. In order to acquire heterogeneously distributed water and minerals[1–3], they optimize their root architecture. One poorly understood plant response to soil phosphate (P_i) deficiency is a reduction in primary root growth with an increase in the number and length of lateral roots[4–12]. Here we show that physical contact of the *Arabidopsis thaliana* primary root tip with low-P_i medium is necessary and sufficient to arrest root growth. We further show that loss-of-function mutations in *Low Phosphate Root1* (*LPR1*) and its close paralog *LPR2* strongly reduce this inhibition. *LPR1* was previously mapped as a major quantitative trait locus (QTL)[12]; the molecular origin of this QTL is explained by the differential allelic expression of *LPR1* in the root cap. These results provide strong evidence for the involvement of the root cap in sensing nutrient deficiency, responding to it, or both. *LPR1* and *LPR2* encode multicopper oxidases (MCOs), highlighting the essential role of MCOs for plant development.

To study the effect of mineral deficiency on root development, we previously mapped *LPR1*, a QTL with a large effect involved in primary root growth arrest in response to low P_i and in the control of primary root cell length[12], in an *A. thaliana* recombinant inbred line (RIL) population derived from the Bay0 (Bayreuth) and Sha (Shahdara) wild accessions. From this RIL population we derived two near isogenic lines (NIL) of line no. 194 (ref. 12). Seedlings of the NIL 194^{Sha}, homozygous for the dominant Sha allele of *LPR1* ($LPR1^{Sha}$), have a short root phenotype on low (5 μM) P_i compared with the NIL 194^{Bay0} carrying the recessive $LPR1^{Bay0}$ allele[12]. We have further shown (**Supplementary Fig. 1a–c** online) that this root growth arrest is related to low P_i, as varying two chemical parameters in the growth medium that affect P_i bioavailability in soils[13]—the pH and the Fe concentration—had an effect on growth arrest (that is, when the medium did not contain Fe or had a more basic pH, the root growth was not inhibited by low P_i).

To determine the molecular basis of the *LPR1* QTL, we identified the responsible gene *LPR1* (At1g23010) by combining several complementary strategies summarized here (see Methods for details). First, by analyzing the existing RIL collection of the Bay0 × Sha cross[14], we mapped the *LPR1* QTL to a 36-kb region of chromosome I (**Supplementary Table 1** online). Second, in order to generate mutant alleles of the *LPR1* QTL, we devised a γ-ray mutagenesis strategy. Radiation induces large deletions as well as point mutations[15]. We therefore used pollen from γ-ray–mutagenized 194^{Sha} plants to pollinate flowers of 194^{Bay0} plants and screened for progeny (F1) seedlings with a long primary root on low P_i. In this way, we isolated three point mutations in the $LPR1^{Sha}$ gene (in addition to 17 large deletion alleles of the $LPR1^{Sha}$ locus), each having a strongly reduced response to low P_i (**Supplementary Fig. 2** online and **Fig. 1a–c**). Two transfer DNA (T-DNA) insertion mutants of At1g23010 (*lpr1-1* and *lpr1-2*, **Fig. 1a**) generated in another genetic background (Col-0)[16], which are most probably null alleles (**Supplementary Fig. 3a,c** online), behaved similarly to the γ-ray–induced mutants (**Fig. 1b,c**), whereas T-DNA mutants in the genes immediately proximal or distal to At1g23010 had a wild-type phenotype (data not shown). Third, the *lpr1-1* T-DNA allele did not genetically complement the $LPR1^{Bay0}$ allele of the QTL (**Supplementary Fig. 4** online). Fourth, a molecular construct containing the $LPR1^{Sha}$ gene restored low-P_i responsiveness to the inbred line 194^{Bay0} (**Fig. 1d**).

A closely related *A. thaliana* paralog of *LPR1*, At1g71040 (hereafter named *LPR2*), has 79% identical amino acids (data not shown). We isolated two T-DNA insertion mutants[16] of *LPR2* (*lpr2-1* and *lpr2-2*) that are most probably null alleles (**Supplementary Fig. 3b,c**). Analysis of the *lpr2* mutants and of the *lpr1-1,lpr2-1* double mutant showed that *LPR1* and *LPR2* had similar and additive roles and were necessary for the root growth response to low P_i (**Fig. 2**).

The predicted amino acid sequences of LPR1 and LPR2 are similar to those of MCOs[17]. In particular, they contain the twelve copper binding amino acids required for MCO catalytic activity in CotA, a structurally characterized MCO of *Bacillus subtilis*[18] (**Fig. 3a**).

[1]Laboratoire de Biologie du Développement des Plantes, Département d'Écophysiologie Végétale et de Microbiologie, Unité Mixte de Recherche 6191 Commissariat à l'Énergie Atomique (CEA), Centre National de la Recherche Scientifique (CNRS), Université Aix-Marseille-II, CEA Cadarache, 13108 St. Paul-lez-Durance Cedex, France. [2]Present address: Equipe Rhizogenese, Unité Mixte de Recherche Diversité et Adaptation des Plantes Cultivées, Institut de Recherche pour le Développement, 911, Avenue Agropolis, 34394 Montpellier Cedex 5, France. [3]Present address: Department of Plant Breeding and Genetics, Max Planck Institute for Plant Breeding Research, Carl-von-Linné-Weg 10, D-50829 Cologne, Germany. [4]Present address: Monsanto, Route de Crest, 26740 Sauzet, France. Correspondence should be addressed to T.D. (thierry.desnos@cea.fr).

Received 20 February; accepted 12 April; published online 13 May 2007; doi:10.1038/ng2041

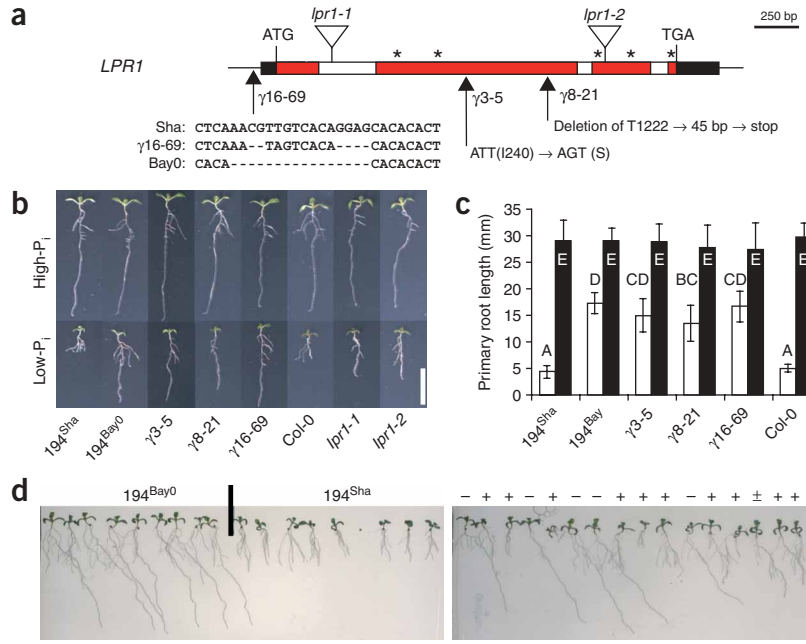

Figure 1 *LPR1* is necessary for root growth inhibition by low P_i. (**a**) Position of the T-DNA insertions (triangles) and γ-ray–induced point mutations (arrows) in *lpr1* alleles. *Copper-binding sites in LPR1 (see text and **Fig. 3**). (**b**) Phenotypes of 194^{Bay0} and 194^{Sha} NILs, the γ-ray induced 194^{Sha} mutants, Col-0 wild-type and the two insertion mutants. Scale bar, 1 cm. (**c**) Histogram of the primary root length of the *lpr1* mutants grown for 9 d on low-P_i (white bars) or high-P_i (black bars) medium (mean ± s.e.m., $n = 4$–14 seedlings). Values with differing letters are significantly different at the $P < 0.05$ level. (**d**) Complementation of NIL 194^{Bay0}. Control lines (left panel) and progeny of a 194^{Bay0} plant segregating for the $LPR1^{Sha}$ transgene (right panel). Seedlings were grown for 9 d on low-P_i medium. +, green fluorescence of seedlings provided by the transformation marker GFP from the transgene; ±, faint fluorescence; –, nonfluorescence.

Accordingly, we observed that *in vitro*, $LPR1^{Sha}$ oxidizes 2,2′-azinobis(3-ethylbenzothiazoline-6-sulfonate) (ABTS), whereas no MCO activity was detected with an $LPR1^{Sha}$ protein containing the γ3-5 mutation or mutated at one putatively crucial copper-binding histidine[19] (**Fig. 3b**). If the MCO activity of the LPR proteins is required for the low P_i–induced root growth arrest, then inhibiting this activity should enhance wild-type root growth. To test this hypothesis, we grew wild-type (Col-0) seedlings on a low-P_i medium supplemented with either 10 μM tetrathiomolybdate (TTM) or 50 μM sodium fluoride (NaF), two potent inhibitors of MCOs[20,21]. At 10 μM TTM, the wild-type primary root was 2.8 times longer than on the TTM-free control medium (respectively 12.4 ± 1.6 mm and 4.4 ± 0.8 mm) and was as long as that of the *lpr1-1* mutant (12.7 ± 1.0 mm) (**Fig. 3c**). Similar results were obtained with NaF (**Fig. 3d**). Thus, phenocopying the Lpr^- mutant phenotype by treating wild-type with TTM or NaF supports the view that MCO activity, most probably resulting from the *LPR1* and *LPR2* expression, is required for low P_i–dependent growth inhibition.

In order to find the molecular origin of the *LPR1* QTL, we first compared the protein sequences of $LPR1^{Bay0}$ and $LPR1^{Sha}$. There are six amino acid substitutions, but these are not in conserved MCO motifs (**Fig. 3a**); and in RIL no. 98 a recombination in exon 2 of *LPR1* (**Supplementary Table 1** and **Fig. 3a**) excluded the possibility that the QTL is in the 3′ half of the gene. Notably, the *in vitro* activity of $LPR1^{Bay0}$ was not significantly different from that of $LPR1^{Sha}$ (**Fig. 3b**). Furthermore, the 194^{Bay0} line was complemented by a transgene containing the $LPR1^{Bay0}$ coding sequence placed under the control of the promoter sequence of $LPR1^{Sha}$ (**Supplementary Fig. 5** online).

Taken together, these data imply that the functional difference between the $LPR1^{Bay0}$ and $LPR1^{Sha}$ alleles is linked to the promoter sequences of *LPR1* (*pLPR1*) rather than to the LPR1 enzymatic activity *per se*.

When compared with $pLPR1^{Sha}$, $pLPR1^{Bay0}$ had several polymorphisms (substitutions, insertions and deletions). However many of these polymorphisms were shared with $pLPR1^{Col-0}$ (data not shown), a functional allele (as shown above). Forty-one nucleotides upstream of the *LPR1* transcription start site, $pLPR1^{Bay0}$ had a 16-bp deletion (**Fig. 1a**). This small part of the promoter region must be crucial for *LPR1* gene function, as the γ-ray–induced allele γ16-69, derived from the $LPR1^{Sha}$ allele, was mutated at this site (**Fig. 1a**) and behaved the same as the γ8–21 allele, which is most probably a null allele (**Fig. 1b**,**c**). These data imply that, compared with $pLPR1^{Sha}$, the function of

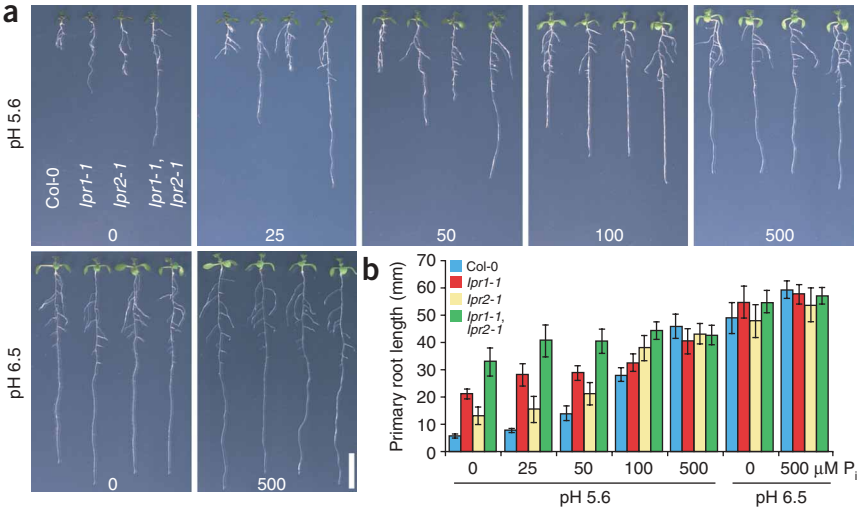

Figure 2 *LPR1* and *LPR2* have similar and additive functions. (**a**) Phenotype of Col-0 wild-type, *lpr1-1* and *lpr2-1* single mutants and *lpr1-1,lpr2-1* double mutants. Seedlings were grown for 9 d on pH-5.6 (top row) or pH-6.5 (bottom row) medium with P_i at the concentrations (μM) indicated at the bottom. The genotypes of the four lines are as in the top left panel. Scale bar, 1 cm. (**b**) Histogram of the primary root length of lines grown as in **a**, mean ± s.e.m., $n = 13$–19 seedlings.

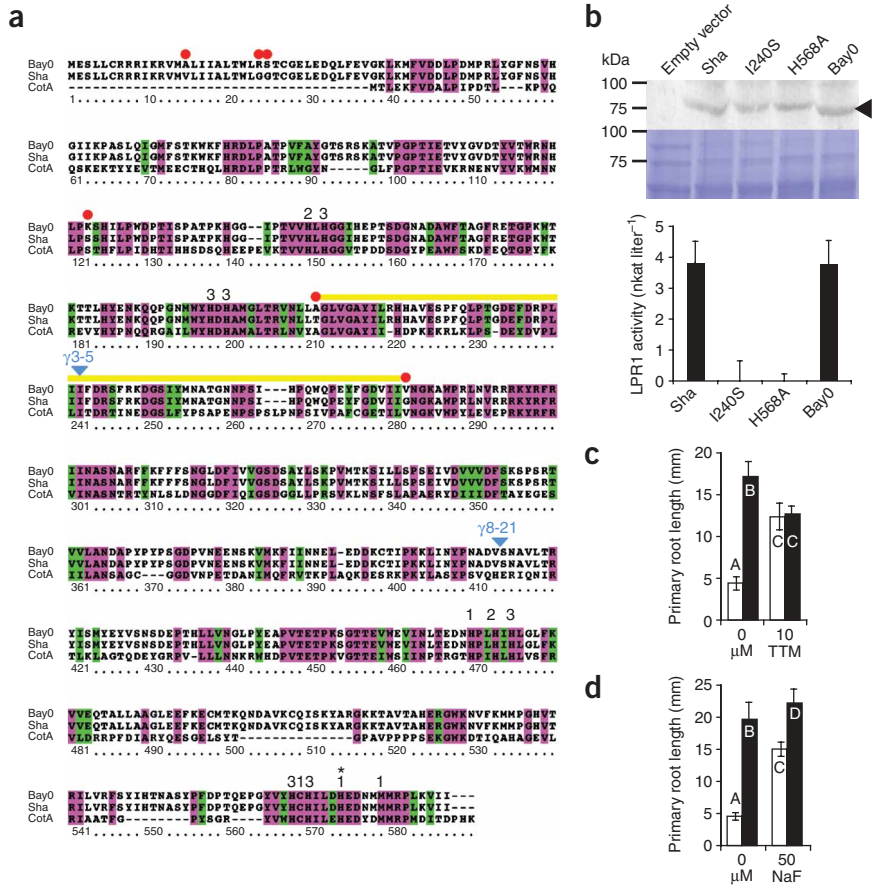

Figure 3 LPR1 is a multicopper oxidase. (**a**) Alignment of LPR1^{Sha} and LPR1^{Bay0} protein sequences with CotA from *Bacillus subtilis*. Red dots, amino acids polymorphic between LPR1^{Sha} and LPR1^{Bay0}; yellow line, region of the crossing over in RIL no. 98; blue arrowheads, positions of the γ3-5 and γ8-21 mutations; numbers above the sequences, amino acids binding the type 1, type 2 or type 3 copper atoms in CotA (ref. 18); *His568. Purple background, amino acids that are identical between LPR1 proteins and CotA; green background, amino acids that are similar. (**b**) MCO activity in protein extracts from yeast strains expressing LPR1^{Sha}, LPR1^{Bay0} or the I240S or H548A mutant forms of LPR1^{Sha}. Above, immunoblot and Coomassie gel of protein extract from yeast strains transformed with empty or LPR1-expressing vector (arrowhead, LPR1). Below, LPR1 catalytic activity; each bar, mean (± s.e.m.) of a triplicate of four independent LPR1 yeast clones minus the activity of the empty-vector control. (**c**,**d**) Inhibitors of MCOs phenocopy the *lpr*$^{-}$ mutant phenotype. Effects of TTM (**c**) and NaF (**d**) on the primary root length of Col-0 wild-type (white bars) and *lpr1-1* (black bars) seedlings grown on a low-P$_i$ medium for 8 days; mean ± s.e.m., $n = 14$ or 15 seedlings (**c**) or $n = 8$–11 seedlings (**d**). Values with differing letters are significantly different at the $P < 0.05$ level.

pLPR1^{Bay0} is somehow less effective, possibly due to less transcription. To test this hypothesis, we analyzed *LPR1* mRNA accumulation in the two NILs 194^{Bay0} and 194^{Sha} by quantitative RT-PCR (QRT-PCR). Both 194^{Bay0} and 194^{Sha} seedlings had *LPR1* mRNA in their roots and leaves. However, *LPR1* mRNA abundance in roots of 194^{Sha} seedlings was 2.5 and 3-fold that in 194^{Bay0}, respectively in low and high P$_i$ (**Fig. 4a** and **Supplementary Fig. 3d**). This is consistent with the recessive nature of the *LPR1^{Bay0}* allele compared with the *LPR1^{Sha}* allele[12].

The 194^{Bay0} seedlings expressed *LPR1* mRNA encoding an active MCO, and yet behaved as a loss-of-function allele (**Fig. 1b**,**c**). In order to understand this apparent paradox, we examined the expression pattern of *LPR1* in more detail. We introduced the transcriptional transgene β-glucuronidase (*GUS*) reporters *pLPR1^{Bay0}::GUS* and *pLPR1^{Sha}::GUS* into the 194^{Bay0} background. *pLPR1^{Sha}::GUS* was expressed in the root tip, including the meristematic region (where root cells are generated) and the root cap (the small group of cells wrapped around the root tip) (**Fig. 4b**). Notably, there was less expression in the root tip of *pLPR1^{Bay0}::GUS* than *pLPR1^{Sha}::GUS*. In particular, there was little, if any, expression of *pLPR1^{Bay0}::GUS* in the root cap (**Fig. 4b**, left panel). We confirmed these results by semiquantitative RT-PCR performed on laser-microdissected root cap tissues (**Fig. 4c**,**d**). These expression patterns were constitutive, as they were not linked to the P$_i$, Fe or H$^+$ concentrations in the growth medium (**Supplementary Fig. 6** online) nor to the genetic backgrounds: in NIL 194^{Sha} the two reporter constructs gave root GUS stainings similar to that in the 194^{Bay0} background (**Supplementary Fig. 6**). Altogether, these data strongly indicate that the molecular basis of the *LPR1* QTL derives from the different patterns of *LPR1* expression in the root tip.

We tested two hypotheses that could explain low P$_i$–dependent root growth arrest: the first posits a nutritional response and the second posits a signaling response. According to the first hypothesis, growth would cease because of internal phosphate deficiency in cells. To test this we measured the P$_i$ content of roots. When grown on low P$_i$ for 10 d, the P$_i$ content of 194^{Sha} and Col-0 wild-type roots was not significantly ($P < 0.05$) different from that of 194^{Bay0} and *lpr1-1* (**Supplementary Table 2** online), indicating that the first hypothesis may be rejected. According to the second hypothesis, root growth arrest would be triggered when the root tip senses the low P$_i$ concentration of the medium. This theory was supported by the result of a compartmented root-growth experiment, in which we found that the primary root-growth arrest occurred when the root tip was in contact with the low-P$_i$ medium, even if leaves were in contact with a high-P$_i$ medium (**Fig. 5**). In another experiment we observed on low-P$_i$ plates that if a primary root tip did not touch the agar medium the root growth was not inhibited, but if, in growing farther, the root tip eventually encountered the medium, then root growth soon ceased (**Supplementary Fig. 7** online). The rapid root growth arrest (less than 2 d) after transfer of Col-0 seedlings from high- to low-P$_i$ media (**Supplementary Fig. 1c**) is also compatible with this second hypothesis. Furthermore, this arrest correlated with the arrest of root cells divisions (**Supplementary Fig. 6** and ref. 10) and elongation[12] and corroborated findings that roots locally sense and respond to low P$_i$[22]. Overall, these results strongly indicate that the root cap is the site of the sensing and/or response to low concentrations of exogenous P$_i$.

In summary, analysis of *A. thaliana* natural variation allowed us to isolate the major QTL *LPR1* controlling low P$_i$–triggered root growth inhibition. This QTL is explained by the differential allelic expression of *LPR1* in the root cap, an organ essential for root meristem

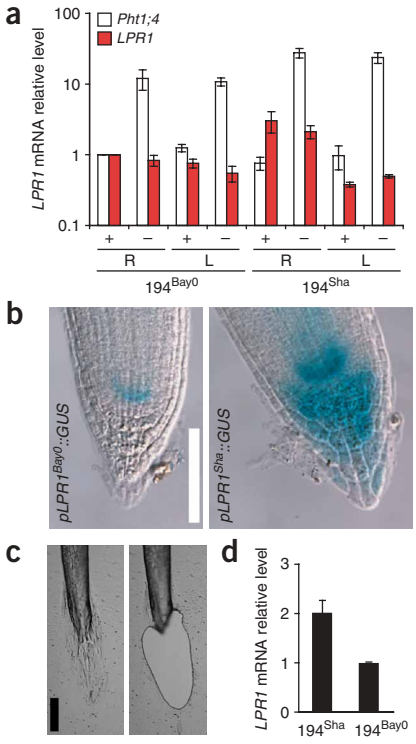

Figure 4 In the root tip, less *LPR1*^{Bay0} than *LPR1*^{Sha} is expressed. (**a**) Histogram of the QRT-PCR analysis of *LPR1* mRNA in leaves (L) and roots (R) of NIL 194^{Bay0} and 194^{Sha} seedlings grown on high P_i (+) or low P_i (–). *Pht1;4* is a low P_i–induced control gene[30]. Mean (± s.e.m.) of a triplicate of three independent QRT-PCR reactions. Data normalized to 194^{Bay0} roots in high P_i. (**b**) GUS staining of the root tips of 194^{Bay0} seedlings carrying the *pLPR1*^{Bay0}*::GUS* (left) or the *pLPR1*^{Sha}*::GUS* (right) construct. Scale bar, 100 µm. (**c**,**d**) *LPR1* mRNA abundance in root cap. (**c**) Root tip before (left) and after (right) laser microdissection of the root cap. Scale bar, 100 µm. (**d**) Semiquantitative RT-PCR analysis of *LPR1* mRNA abundance in the microdissected root caps of 194^{Sha} and 194^{Bay0} seedlings. Data normalized to 194^{Bay0}; mean ± s.e.m. ($n = 3$).

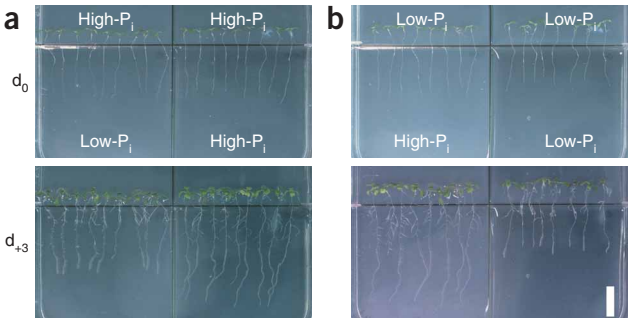

Figure 5 Root growth on low-P_i medium is inhibited through the root tip. Col-0 wild-type seedlings first grown for 3 d on a high-P_i medium (not shown here) and then transferred at day 0 (d_0) to the indicated compartmentalized vertical plates such that the upper and lower parts of each seedling were in contact with different media. (**a**) Upper part of the seedlings on high-P_i medium, lower part on low-P_i or high-P_i medium. (**b**) Upper part of the seedlings on low-P_i medium, lower part on high-P_i or low-P_i medium. Lower panels, the same plates 3 d later (d_{+3}). Scale bar, 2.5 mm.

maintenance[23] and auxin fluxes[24]. We propose that when the primary root tip reaches a low-P_i zone, the LPR proteins of the root cap modify the activity and/or distribution of a hormone-like compound. This triggers the primary root developmental switch from indeterminate to determinate growth[10], the reduction of cell elongation and the promotion of lateral roots. This is the first demonstration that MCOs have a role in plant development in response to an abiotic signal. As both prokaryotes and eukaryotes harbor MCOs[25], these findings may contribute to understanding other developmental processes.

METHODS

Plant material and growth conditions. The SALK lines[16] were provided by the Nottingham *Arabidopsis* Stock Centre. For the QTL fine mapping we used the 411-RIL population previously described[14] (see http://dbsgap.versailles.inra.fr/vnat/ for details). Seedling and plant growth conditions were as previously described[12]. The 194^{Sha} and 194^{Bay0} lines are NILs with, respectively, a Sha or a Bay0 allele in the MSAT1.10–nga248 region[12]. Unless otherwise indicated, the growth medium was buffered at pH 5.6 with 3.5 mM 2-(*N*-morpholino)ethane sulfonic acid (MES) buffer before autoclaving. The ammonium tetrathiomolybdate was from Aldrich and NaF from Prolabo.

Fine mapping of *LPR1*. We screened the population of 411 RILs for lines carrying a recombinant chromosome in the 2.6-Mb interval flanked by the molecular markers MSAT1.10 and nga248. We selected 48 RILs and phenotyped them in low-P_i conditions, and fine-mapped the recombination breakpoints with newly developed microsatellite markers (**Supplementary Tables 1** and **3** online), allowing us to localize *LPR1* to a 56-kb interval. We then narrowed *LPR1* down to a 38-kb interval by sequencing DNA of two RILs with recombination breakpoints in close proximity to *LPR1* (**Supplementary Table 1**). See **Supplementary Methods** online for further details.

Gamma-ray mutagenesis and identification of the *lpr1* γ-mutants. Eight flowering 194^{Sha}/194^{Sha} plants were exposed to 200 Gy (17 Gy min^{-1}) of γ-rays from a ^{60}Co source. We used the irradiated pollen to manually pollinate the castrated flowers of nineteen 194^{Bay0}/194^{Bay0} plants, and sowed ~11,000 resulting F1 seeds on low-P_i plates. In the 51 putative *lpr1* F1 mutants, we mapped the γ-ray–induced deletions with PCR markers located between MSAT1.10 and nga248 (**Supplementary Fig. 2**). In four F1 plants we did not detect large deletions; in their F2 progeny we selected seedlings homozygous for the Sha allele using PCR markers in the *LPR1* region and sequenced the At1g23010 gene. The sequence of each point mutation was verified in a second mutant sibling. See **Supplementary Methods** for further details.

Molecular constructs. For complementation, we PCR-amplified from genomic DNA the At1g23010 gene of the Sha accession, including 2.1 kb upstream of the ATG and 245 bp downstream of the stop codon, and cloned it into the pFP100 vector (http://www.isv.cnrs-gif.fr/jg/), yielding the *LPR1*^{Sha}-pFP100 construct.

For the promoter-GUS fusion, we amplified from genomic DNA a 2.1-kb fragment upstream of the ATG of the At1g23010 gene from the 194^{Bay0} and 194^{Sha} lines and cloned it in a pXCSG-GFP–derived vector[26] (L. Noël, CEA Cadarache, unpublished data) in which the *GFP* gene was replaced by the *GUS* gene, yielding the *pLPR1*^{Bay0}*::GUS* and *pLPR1*^{Sha}*::GUS* constructs, respectively.

These different constructs were introduced[27] into the 194^{Bay0} and 194^{Sha} lines and transformants were selected either under UV light for the *LPR1*^{Sha}-pFP100 construct or by BASTA (AgrEvo) selection in soil for the other constructs. See **Supplementary Methods** and **Supplementary Table 3** for further details.

Real-time QRT-PCR. We carried out real-time QRT-PCR using an ABI 7000 (Applied Biosystems) with SYBR Premix ExTaq (Perfect Real Time) as in ref. 28. Standard curves were generated by serial dilutions of first-strand cDNA preparations.

Laser microdissection of root caps and semiquantitative RT-PCR. We grew 194^{Bay0} and 194^{Sha} seedlings 7 d on a high-P_i medium and then cut their primary roots and directly deposited the roots on the plastic film of laser microdissection slides (Leica). We performed the microdissections under a

LMD6000 (Leica) microscope. For each line, ~80 root caps were collected in 75 µl of RNA extraction buffer containing 10 mM DTT; tubes were then stored at –80 °C. Total RNA was extracted with the RNeasy Micro Kit (50) (Qiagen) according to the manufacturer's instructions and eluted in 14 µl RNase-free water. First-strand cDNA synthesis is described in the **Supplementary Methods**. Semiquantitative RT-PCR was performed on an *ep*-gradient-S thermocycler (Eppendorf) and the relative expression of *LPR1* mRNA was normalized to the amount of the root cap–specific *CEL5* mRNA[29].

GUS staining. We selected lines which gave a 3:1 segregation of kanamycin resistance (carried by the T-DNA) and grew them for 9 d on a high-P_i medium. GUS staining of plant tissues was performed as previously described[29] except that seedlings were incubated in the staining solution for 6 h and then treated with 70% ethanol at 55 °C for 1 h. GUS staining was repeated four times each with two independent lines for each construct, $n = \sim 10$ seedlings per line. These four experiments gave similar results.

LPR1 MCO activity. Wild-type and mutant LPR1 proteins were produced in *Saccharomyces cerevisiae* and the MCO activity assayed on ABTS with total protein extracts (**Supplementary Methods**).

Immunoblotting. Yeast protein extracts were separated by SDS-PAGE and blotted. The membrane was soaked with a polyclonal antibody to CotA (see Acknowledgments) and stained with an alkaline phosphatase–conjugated goat antibody to rabbit IgG (Sigma).

Accession codes. Genbank: $LPR1^{Bay0}$ coding sequence, DQ663631; $LPR1^{Sha}$ coding sequence, DQ663632. PDB: CotA, 1GSK. *Arabidopsis thaliana*: Bay0, N57923; Sha, N57924; Columbia (Col-0), CS60000; *lpr1-1*, SALK_016297; *lpr1-2*, SALK_050267; *lpr2-1*, SALK_091930; *lpr2-2*, SALK_061362.

Note: Supplementary information is available on the Nature Genetics website.

ACKNOWLEDGMENTS

We gratefully thank the Nottingham *Arabidopsis* Stock Centre for providing SALK insertion lines; J. Vicente for the γ-ray irradiation; L. Martins (Instituto de Tecnologia Química e Biológica, Oeiras) for the CotA antibody; L. Noël (CEA Cadarache) for the pXCSG-GFP vector; F. Parcy (CNRS, Grenoble) for the pFP100 vector; T. Tron (CNRS, Marseille) for the yeast vectors; N. Leonhardt for helping with QRT-PCR; C. Sallaud for the 96-well DNA extraction protocol; A. Caroff for helping with laser microdissection; C. Sarrobert for her early involvement on Fe studies; the Groupement de Recherches Appliquées en Phytotechnologie team for taking care of plants; J.-L. Montillet for helpful discussions; and M. Crespi, M. Koornneef, G. Kunze, E. Marin-Nussaume, L. Noël and M.-C. Thibaud for critical reading and suggestions on an early version of the manuscript. We thank R. Carol for correcting the English on an early version of the manuscript. S.S. was supported by the French Ministère de la Recherche and by the CEA; C.S.-C., M.R. and L.R. were supported by the CEA.

AUTHOR CONTRIBUTIONS

S.S., A.C. and T.D. performed most of the experiments. M.R. contributed to the fine mapping of *LPR1* and performed statistical analysis; C.S.-C. performed enzymatic analysis of LPR1; L.R. complemented the 194^{Bay0} line; A.B. isolated the *lpr2* mutants. S.S. and T.D. analyzed the data and wrote the manuscript with input from L.N. T.D. conceived and supervised the project.

COMPETING INTERESTS STATEMENT

The authors declare no competing financial interests.

Published online at http://www.nature.com/naturegenetics
Reprints and permissions information is available online at http://npg.nature.com/reprintsandpermissions

1. Forde, B. & Lorenzo, H. The nutritional control of root development. *Plant Soil* **232**, 51–68 (2001).
2. Lopez-Bucio, J., Cruz-Ramirez, A. & Herrera-Estrella, L. The role of nutrient availability in regulating root architecture. *Curr. Opin. Plant Biol.* **6**, 280–287 (2003).
3. Malamy, J.E. Intrinsic and environmental response pathways that regulate root system architecture. *Plant Cell Environ.* **28**, 67–77 (2005).
4. Raghothama, K.G. Phosphate acquisition. *Annu. Rev. Plant Physiol. Plant Mol. Biol.* **50**, 665–693 (1999).
5. Lynch, J.P. & Brown, K.M. Topsoil foraging—an architectural adaptation of plants to low phosphorus availability. *Plant Soil* **237**, 225–237 (2001).
6. Williamson, L.C., Ribrioux, S.P., Fitter, A.H. & Leyser, H.M. Phosphate availability regulates root system architecture in *Arabidopsis*. *Plant Physiol.* **126**, 875–882 (2001).
7. López-Bucio, J. *et al.* Phosphate availability alters architecture and causes changes in hormone sensitivity in the *Arabidopsis* root system. *Plant Physiol.* **129**, 244–256 (2002).
8. Chevalier, F. *et al.* Effects of phosphate availability on the root system architecture: large-scale analysis of the natural variation between *Arabidopsis* accessions. *Plant Cell Environ.* **26**, 1839–1850 (2003).
9. Ticconi, C.A. & Abel, S. Short on phosphate: plant surveillance and countermeasures. *Trends Plant Sci.* **9**, 548–555 (2004).
10. Sánchez-Calderón, L. *et al.* Phosphate starvation induces a determinate developmental program in the roots of *Arabidopsis thaliana*. *Plant Cell Physiol.* **46**, 174–184 (2005).
11. Sánchez-Calderón, L. *et al.* Characterization of *low phosphorus insensitive* (*lpi*) mutants reveals a crosstalk between low P-induced determinate root development and the activation of genes involved in the adaptation of *Arabidopsis* to P deficiency. *Plant Physiol.* **140**, 879–889 (2006).
12. Reymond, M., Svistoonoff, S., Loudet, L., Nussaume, L. & Desnos, T. Identification of QTL controlling root growth response to phosphate starvation in *Arabidopsis thaliana*. *Plant Cell Environ.* **29**, 115–125 (2006).
13. Hinsinger, P. Bioavailability of soil inorganic P in the rhizosphere as affected by root-induced chemical changes: a review. *Plant Soil* **237**, 173–195 (2001).
14. Loudet, O., Chaillou, S., Camilleri, C., Bouchez, D. & Daniel-Vedele, F. Bay-0 × Shahdara recombinant inbred line population: a powerful tool for the genetic dissection of complex traits in *Arabidopsis*. *Theor. Appl. Genet.* **104**, 1173–1184 (2002).
15. Naito, K. *et al.* Transmissible and nontransmissible mutations induced by irradiating *Arabidopsis thaliana* pollen with γ-rays and carbon ions. *Genetics* **169**, 881–889 (2005).
16. Alonso, J.M. *et al.* Genome-wide insertional mutagenesis of *Arabidopsis thaliana*. *Science* **301**, 653–657 (2003).
17. Solomon, E.I., Sundaram, U.M. & Machonkin, T.E. Multicopper oxidases and oxygenases. *Chem. Rev.* **96**, 2563–2605 (1996).
18. Enguita, F.J., Martins, L.O., Henriques, A.O. & Carrondo, M.A. Crystal structure of a bacterial endospore coat component. *J. Biol. Chem.* **278**, 19416–19425 (2003).
19. Martins, L.O. *et al.* Molecular and biochemical characterization of a highly stable bacterial laccase that occurs as a structural component of the *Bacillus subtilis* endospore coat. *J. Biol. Chem.* **277**, 18849–18859 (2002).
20. Chidambaram, M.V., Barnes, G. & Frieden, E. Inhibition of ceruloplasmin and other copper oxidases by thiomolybdate. *J. Inorg. Biochem.* **22**, 231–240 (1984).
21. Curzon, G. The effects of ions and chelating agents on the oxidase activity of ceruloplasmin. *Biochem. J.* **77**, 66–73 (1960).
22. Franco-Zorrilla, J.M., Martin, A.C., Leyva, A. & Paz-Ares, J. Interaction between phosphate-starvation, sugar, and cytokinin signaling in *Arabidopsis* and the roles of cytokinin receptors CRE1/AHK4 and AHK3. *Plant Physiol.* **138**, 847–857 (2005).
23. Tsugeki, R. & Fedoroff, N.V. Genetic ablation of root cap cells in *Arabidopsis*. *Proc. Natl. Acad. Sci. USA* **96**, 12941–12946 (1999).
24. Kramer, E.M. & Bennett, M.J. Auxin transport: a field in flux. *Trends Plant Sci.* **11**, 382–386 (2006).
25. Nakamura, K. & Go, N. Function and molecular evolution of multicopper blue proteins. *Cell. Mol. Life Sci.* **62**, 2050–2066 (2005).
26. Witte, C.P. *et al.* Rapid one-step protein purification from plant material using the eight-amino acid StrepII epitope. *Plant Mol. Biol.* **55**, 135–147 (2004).
27. Clough, S.J. & Bent, A.F. Floral dip: a simplified method for *Agrobacterium*-mediated transformation of *Arabidopsis* thaliana. *Plant J.* **16**, 735–743 (1998).
28. Herbette, S. *et al.* Genome-wide transcriptome profiling of the early cadmium response of *Arabidopsis* roots and shoots. *Biochimie* **88**, 1751–1765 (2006).
29. del Campillo, E., Abdel-Aziz, A., Crawford, D. & Patterson, S.E. Root cap specific expression of an endo-β-1,4-D-glucanase (cellulase): a new marker to study root development in *Arabidopsis*. *Plant Mol. Biol.* **56**, 309–323 (2004).
30. Misson, J., Thibaud, M.-T., Bechtold, N., Raghothama, K. & Nussaume, L. Transcriptional regulation and functional properties of *Arabidopsis* Pht1;4, a high affinity transporter contributing greatly to phosphate uptake in phosphate deprived plants. *Plant Mol. Biol.* **55**, 727–741 (2004).